IJST, Transactions of Mechanical Engineering, Vol. 39, No. M1, pp 1-14
Printed in The Islamic Republic of Iran, 2015

AN EXTENDED CONTINUUM MECHANICS FORMULATION ENHANCED BY DIRECT COUPLING WITH MOLECULAR DYNAMICS*

S. E. HABIBI**[1], M. FARID[2], M. H. KADIVAR[3] AND M. MAHZOON[4]

[1]Dept. of Mechanical Engineering, Persian Gulf University, Bushehr, I. R. of Iran
Email: habibie@pgu.ac.ir
[2-4]School of Mechanical Engineering, College of Engineering, Shiraz University, Shiraz, I. R. of Iran

Abstract– Based on the notion of micro-structure in linear elasticity presented by Mindlin, a new extended continuum mechanics (ECM) formulation is derived which can be utilized to model the material behavior at atomic scale. An attempt has been made to present a formulation capable of producing the molecular dynamics (MD) simulation results with less computational effort. To this end, some new kinematical variables are defined and some constitutive relations are obtained from MD. To validate the proposed ECM formulation, it is applied to a properly defined sample problem and the response is compared with the MD simulation result and the classical continuum mechanics (CCM) solution.

Keywords– Extended continuum mechanics (ECM), generalized continua, molecular dynamics, nanomechanics, dipolar continuum mechanics

1. INTRODUCTION

Extended continuum mechanics (ECM) theories refer to the extension of the classical continuum mechanics (CCM) in microscopic space and short time scales. A material body may be envisioned as a collection of large number of deformable particles that contribute to the macroscopic behavior of the body [1]. Cosserat brothers [2] proposed a systematic development of the mechanics of continuous media, even though the seminal idea was previously presented by Voigt [3]. They considered each material point as a small rigid body which is able to rotate freely with respect to the neighboring material elements. This point of view constituted the first change of the traditional Cauchy's paradigm on the description of the morphology of deformable bodies [4, 5]. Toupin [6] presented a continuum theory in which, in contrast with Cauchy paradigm, couple-stresses are included to the internal interactions. Mindlin [7] established a theory for an elastic solid in which each material point was considered as a deformable media. In the same year, Eringen and Suhubi [8, 9] proposed the theory of nonlinear microelastic continuum. Materials well described by Mindlin's model were named micromorphic materials by Eringen and Suhubi. Green and Rivlin [10, 11] introduced higher-order micromorphic continua.

The ability of existing ECM theories to predict the atomic structural behavior was examined by Chen et al. [12-15]. They concluded that although the micromorphic theory and the nonlocal theory of elasticity are the best candidates to give a corresponding response with the atomistic lattice dynamics and MD, these theories, at best, can only predict the time averaged values of molecular dynamic simulation results and no available ECM formulation is able to predict the instantaneous atomic response, e.g. atomic vibration. Multiscale continuum field theories in which the atomic data are injected in field equations by homogenization or statistical averaging of nano-scale variables have been used extensively [16-18].

*Received by the editors September 29, 2013; Accepted July 22, 2014.
**Corresponding author

Recently, the ability of generalized continuum theories to capture dispersion characteristics at the atomic scale has been investigated [19]. It was shown that only certain models with specific kernel functions are able to follow dispersion curve of Borne-Karman's atomic model [19]. The main drawback of the available ECM formulism is that due to the lack of concurrent coupling with the atomic scale response, the resulted formulation can only predict the time averaged behavior of nano-scale materials [17]. It was pointed out that the classical continuum mechanics with some improvements is enough for a sufficient description of the mechanical behavior of nano-materials in many situations [20], however, there is clear evidence that the response of nano-scale materials violates the predictions of the continuum models [21]. The sub nanometer wavelength periodic rippling of suspended graphene nano-membranes has been investigated using scanning tunnelling microscopy in [21]. Authors observed that as a result of special interactions between adjacent atoms, the atomic membrane has almost no resistance against out-of-plane deformations. This behavior is in sharp contrast with the phenomenology captured by the continuum plate, where the bending of a plate always induces the in-plane stretching and compression on the opposite sides of a neutral curved surface. Therefore, the malfunctioning of the continuum model goes beyond the issue of selecting an appropriate continuum formulation. Nevertheless, microscopic simulations based on a quantum mechanical description of the chemical binding, accurately describe the observed rippling mode and elucidate the origin of the continuum model breakdown [21]. Thus, it is expected that the concurrent coupling of the continuum formulism with modeling methods taking into account quantum effects may be able to give much better prediction.

Accordingly, the present work is aimed to propose a general structure of a well-defined ECM theory in order to design a methodology for coupling the continuum mechanics with discrete methods such as MD. The desired formulation should be able to model not only the time average values of MD results but also the instantaneous ones. It is worth mentioning that due to the Brownian motion of atoms, exact prediction of these movements is neither possible nor desirable. But, due to their important contributions in material behaviors such as direction and path of crack growth or effects on the wave propagation characteristics of the material, it is very helpful to have a measure of their magnitude.

2. CONFIGURATION AND DEFORMATION

In classical continuum paradigm, the atomic degrees of freedom are removed and replaced by properly defined continuum field averages such as temperature, internal energy, stress and strain. In order to extend this paradigm to incorporate the material sub-structure, each material point referred to as macro-element, is endowed with an abstract space attached to it. More precisely, embedded in each material particle, it is assumed there exists a micro-volume V' called micro-element. Consider a macro-element P in the reference configuration κ_R. We assign a micro-volume V' to each macro element P. The sub-structure particles of the material, which are ignored in the classical continuum mechanics, are placed in this micro-volume in a proper structure according to the macro physical state (e.g. temperature) of the reference configuration. The reference frame X' is placed at the centroid of V' (Fig. 1). Accordingly, each sub-structure particle can be endowed with three rectangular components $\mathrm{X}'_{\mathrm{i}}, \mathrm{i} = 1,2,3$ in the three-dimensional Euclidean space $\mathcal{E}$. To specify the reference configuration of body $\mathfrak{B}$, two sets of coordinates $\mathbf{X}$ and $\mathbf{X}'_{\mathbf{X}}$ must be addressed. Dependence of $\mathbf{X}'_{\mathbf{X}}$ on $\mathbf{P}$ declares that $\mathbf{X}'_{\mathbf{X}}$ is a function of macro placement and physical state conditions of the material point $\mathbf{P}$. To emphasize this dependence, a subscript $\mathbf{X}$ is used in $\mathbf{X}'_{\mathbf{X}}$. Therefore, the reference configuration of $\mathfrak{B}$ can be fully described by two sets of coordinates X_{i} and $\mathrm{X}'_{\mathrm{X}_{\mathrm{i}}}$ and we can write mathematically

$$\mathcal{K}_{\mathrm{R}}: \mathfrak{B} \to \mathcal{E} \times \Re_{\mathrm{P}}, \qquad (\mathrm{X}, \mathrm{X}'_{\mathrm{X}}) \in (\mathcal{E} \times \Re_{\mathrm{P}}), \qquad \mathrm{X}'_{\mathrm{X}_{\mathrm{i}}} = \mathrm{X}'_{\mathrm{X}_{\mathrm{i}}}\left(\mathrm{X}_{\mathrm{j}}, \theta, \ldots\right) \tag{1}$$

where $\Re_P$ and θ denote abstract attached manifold and the temperature at point **P**, respectively.

At each time, $\mathfrak{B}$ takes the configuration χ, with the new macro and micro placements $\boldsymbol{x}$ and $\boldsymbol{x'}_{\mathbf{X}}$, respectively. Accordingly, the macro and micro displacements can also be defined as:

$$u_i = x_i - X_i\,,\ i = 1,2,3. \tag{2-a}$$

$$u'_{x_i} = x'_{x_i} - X'_{X_i}\ ,\ i = 1,2,3, \tag{2-b}$$

in which

$$\chi_i = \chi_i(X_j, t), \qquad i,j = 1,2,3. \tag{3-a}$$

$$x'_{X_i} = \chi'_i\left(X_{X_j}, X_j, \theta, \dots, t\right), \qquad i,j = 1,2,3, \tag{3-b}$$

where χ_i and χ'_i are called macro and micro deformation functions, respectively. These mapping functions are assumed to be invertible and differentiable as many times as desired with respect to both **X** and t. For brevity, the **X** subscript with the primed variables is omitted hereafter.

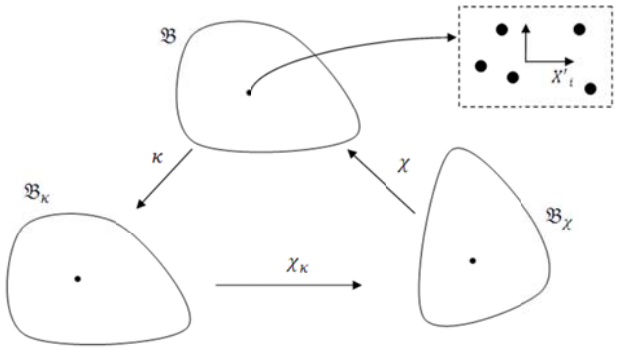

Fig. 1. Schematic representation of structured continuum in different configurations

It is more desirable to define some average properties in micro-volume and assign them to the macro particle. This goal can be achieved by expanding $\mathbf{u}'$ with respect to X'_i about $X'_i = 0$ assuming infinitesimal micro deformations.

$$u'_i(X, X', t, \theta, \dots) = u'_i(X, 0, t, \theta, \dots) + \frac{\partial u'_i}{\partial X'_j}\Big|_{x'=0} X'_j + \cdots . \tag{4}$$

Since $x'_i(X, 0, t, \theta, \dots) = X'_i(X, 0, t, \theta, \dots) = 0$,

$$u'_i(X, X', t, \theta, \dots) = \psi_{ij}(X, t, \theta, \dots)X'_j, \tag{5}$$

where $\psi_{ij}(X, t, \theta, \dots) \triangleq \frac{\partial u'_i}{\partial X'_j}\Big|_{x'=0}$.

As it can be seen ψ_{ij} depends on macro variables and can be regarded as a material property of the macro particle.

3. DERIVATION OF THE BASIC FIELD EQUATIONS

a) Conservation of mass

Consider a configuration κ of the body $\mathfrak{B}$ at time t in which $\mathfrak{B}$ occupies region $\mathcal{R}$ bounded by a closed surface $\partial\mathcal{R}$. Each part (or subset) S of the body $\mathfrak{B}$ is assumed to be endowed with two positive measures M(S) and M′(S), called the macro and micro masses of the part S. Assuming that these measures are absolutely continuous, the following limits can be defined

$$\rho(x, t) = \lim_{V\to 0} \frac{M}{V}, \tag{6-a}$$

$$\rho'(x,\mathrm{t}) = \lim_{\mathrm{V}\to 0} \frac{\mathrm{M}'}{\mathrm{V}}, \tag{6-b}$$

where V is the macro volume considered for the subset S. Two scalars ρ and ρ' are called macro and micro mass densities, respectively. It is noteworthy that assigning the micro mass density to each point of the continuum does not mean that an additional mass is assigned to each particle. In fact, as will be discussed under the definition of the kinetic energy, the micro mass is considered to model the effects of movements of sub-structure particles. These movements are naturally ignored in the CCM.
Material form of the principle of conservation of mass can be presented as follows:

$$(\rho_0 + \rho_0')\,\mathrm{dV} = (\rho + \rho')\,\mathrm{dv}, \tag{7}$$

where variables with subscript zero refer to the referential variables.

b) Conservation of linear momentum

To obtain the governing equations of motion, one straightforward method is to use energy concepts. In the present work an attempt is made to put no specific assumption on the behavior of the micro-kinematical variables. To achieve this goal, in accordance with the Mindlin's approach [7], the variational method is utilized merely to derive the equation of linear momentum.

c) Variational method

We consider T, U and δW as the total kinetic energy of the body, the potential energy of the deformation and the virtual work done by external forces during a virtual displacement, respectively. The kinetic energy of a differential macro-volume dV consists of two parts. The first part is the kinetic energy of the mass ρdV with the translational velocity components $\dot{u}_i$. The second part, which is ignored in CCM theory, is incorporated to include the kinetic energy of moving sub-structure particles. Therefore, the total kinetic energy of a differential macro volume of a generalized continuum can be written as

$$\mathrm{dT} = \frac{1}{2}\rho\dot{\mathrm{u}}_\mathrm{i}\dot{\mathrm{u}}_\mathrm{i}\mathrm{dV} + \sum_\alpha^\mathrm{N}\frac{1}{2}\mathrm{m}^\alpha\left(\dot{\mathrm{u}}_\mathrm{i} + \dot{\mathrm{u}}'^{\alpha}_{\mathrm{i}}\right)\left(\dot{\mathrm{u}}_\mathrm{i} + \dot{\mathrm{u}}'^{\alpha}_{\mathrm{i}}\right), \tag{8}$$

where α runs over the total numbers N of constitutive sub-structure particles embedded in the micro-volume V' and m^α denotes the mass of the α-th particle. It can be assumed that the micro kinetic energy has the same volumetric rate in macro and micro-spaces. Thus, the kinetic energy of the macro-element of the generalized continuum can be simplified as

$$\mathrm{dT} = \left[\frac{1}{2}\rho\dot{\mathrm{u}}_\mathrm{i}\dot{\mathrm{u}}_\mathrm{i} + \frac{1}{\mathrm{V}'}\sum_\alpha^\mathrm{N}\frac{1}{2}\mathrm{m}^\alpha\left(\dot{\mathrm{u}}_\mathrm{i} + \dot{\mathrm{u}}'^{\alpha}_{\mathrm{i}}\right)\left(\dot{\mathrm{u}}_\mathrm{i} + \dot{\mathrm{u}}'^{\alpha}_{\mathrm{i}}\right)\right]\mathrm{dV}, \quad \mathrm{i} = 1,2,3. \tag{9}$$

Introducing micro mass density $\rho' \triangleq \frac{\sum_\alpha^\mathrm{N}\mathrm{m}^\alpha}{\mathrm{V}'}$ and micro inertia density $\mathrm{I_{jk}} \triangleq \frac{\sum_{\alpha_2}^{\mathrm{N}1}\mathrm{m}^\alpha \mathrm{X}_\mathrm{j}'^{\alpha}\mathrm{X}_\mathrm{k}'^{\alpha}}{\mathrm{V}'}$ the total kinetic energy of the generalized continua confined to domain R is the subsequent volume integral.

$$\mathrm{T} = \int_\mathrm{R}\left[\frac{1}{2}\dot{\mathrm{u}}_\mathrm{i}\dot{\mathrm{u}}_\mathrm{i}(\rho + \rho') + \frac{1}{2}\mathrm{I_{jk}}\dot{\psi}_\mathrm{ij}\dot{\psi}_\mathrm{ik}\right]\mathrm{dV}\,. \tag{10}$$

One of the most important parts of the present ECM formulation is the assumed form for various internal interactions in the continua. Macro and micro structural events consist of interactions taking place at macro and micro scales. In addition, each scale imposes some effects on the other one. The virtual work done by these internal actions during a virtual displacement is called virtual stress work. The present framework which provides the possibility of utilizing MD simulation results in ECM formulation is quite flexible and various forms for the virtual stress work can be assumed. In what follows, an assumed form for the virtual stress work is presented and all governing equations are derived accordingly.

$$\delta\mathrm{W}^{\mathrm{in}} = \mathrm{T_{ji}}\,\delta\mathrm{F_{ij}} + \sigma'_{\mathrm{ji}}\,\delta\mathrm{F_{ij}} + \sigma_{\mathrm{ij}}\,\delta\psi_{\mathrm{ij}}. \tag{11}$$

δW^{in} is the virtual stress work per unit macro volume. T_{ji} and F_{ij} are components of macro stress and macro deformation gradient tensors, respectively. The components of the macro deformation gradient tensor are

$$F_{ij} = \frac{\partial u_i}{\partial X_j} = u_{i,j} \quad . \tag{12}$$

Integrating the Eq. (11) between times t_1 and t_2 and simplifying, we have

$$\int_{t_1}^{t_2} \delta W^{in}\, dt =$$

$$\int_{t_1}^{t_2} \left[- \int_R (T_{ji} + \sigma'_{ji})_{,j}\, \delta u_i\, dV + \int_{\partial R} (T_{ji} + \sigma'_{ji}) n_j\, \delta u_i\, ds \right] dt + \int_{t_1}^{t_2} \int_R \sigma_{ij}\, \delta \psi_{ij}\, dV dt. \tag{13}$$

The external action on each particle of the continuum consists of two parts: the body force per unit macro mass **b** and the contact force per unit macro surface area **t**. Therefore the virtual work done by external forces is

$$\delta W = \int_R \rho b_i \delta u_i dV + \int_{\partial R} t_i \delta u_i ds. \tag{14}$$

Accordingly, the equations of motion and related boundary conditions take the following forms

$$(T_{ji} + \sigma'_{ji})_{,j} + \rho b_i = \frac{D}{Dt}[(\rho + \rho')\dot{u}_i] \tag{15-a}$$

$$\sigma_{ji} = -\frac{D}{Dt}(I_{jk}\dot{\psi}_{ik}). \tag{15-b}$$

$$t_i = (\sigma'_{ji} + T_{ji}) n_j \qquad \text{on } \partial R. \tag{15-c}$$

d) Conservation of angular momentum

The total moment of forces acting on the body with respect to the origin of the coordinate system can be represented by

$$m = \int_R \boldsymbol{x} \times \rho \mathbf{b}\, dV + \int_{\partial R} \boldsymbol{x} \times \mathbf{t}\, ds. \tag{16}$$

By adopting the definition (16), the effects of any spin of material particles on the total moment of forces are neglected. Using Euler's second law and applying material derivative and simplifying the results using Eq. (15-a) the local form of the conservation of angular momentum is obtained as follows:

$$\epsilon_{ijk}(T_{ij} + \sigma'_{ij}) = 0. \tag{17}$$

As can be seen, in contrast with assuming non-polar media, macro and micro stress tensors are not necessarily symmetric.

e) Energy equation

Let $\bar{\mathcal{E}}$, r, and q_i stand for total internal energy, heat supply per unit mass and heat flux in the i-th direction on an infinitesimal surface with unit normal vector **n**, respectively. Then, the general form of the energy equation can be written as

$$\frac{D}{Dt}(T + \bar{\mathcal{E}}) = \int_R \rho b_i \dot{u}_i dV + \int_{\partial R} t_i^n \dot{u}_i ds + \int_R \rho r dV - \int_{\partial R} q_i n_i ds. \tag{18}$$

Using Eqs. (10) and (15), and denoting the internal energy per unit volume by ε, after simplification we have

$$\frac{D\varepsilon}{Dt} = (T_{ji} + \sigma'_{ji})\dot{u}_{i,j} + \sigma_{ji}\dot{\psi}_{ij} + \rho r - q_{i,i}. \tag{19}$$

This is the general local form of the equation of conservation of energy for the generalized continuum.

f) Constitutive relations and entropy inequality

As declared by Coleman and Noll [22] entropy inequality places some constraints on the form of constitutive relations. The set of variables $\{F_{ij}, \psi_{ij}, \theta\ (\text{or}\ \eta), X, t\}$ can be selected as independent constitutive variables. To have a consistent theory, the constitutive relations must be defined for the dependent constitutive variables $\{T_{ij}, \sigma_{ij}, \sigma'_{ij}, q_i, \eta\ (\text{or}\ \theta), \varepsilon\ (\text{or}\ \Psi)\}$ as functions of independent ones, in which, η stands for entropy. The entropy inequality in the form of Clausius-Duhem inequality has the following form:

$$\rho\dot{\eta} + \text{div}\left(\frac{q}{\theta}\right) - \frac{\rho r}{\theta} \geq 0. \tag{20}$$

Defining the Helmholtz free energy density as $\Psi \triangleq \varepsilon - \eta\theta$ and assuming the constitutive relation for dependent variable as

$$\{T_{ij}, \sigma_{ij}, \sigma'_{ij}, q_i, \eta\ (\text{or}\ \theta), \varepsilon\ (\text{or}\ \Psi)\} = \mathcal{F}(\{F_{ij}, \theta(\text{or}\ \eta), (\nabla\theta)_i, \psi_{ij}\}) \tag{21}$$

and using some mathematical manipulations Eq. (20) is rendered as:

$$\rho\dot{\theta}\left(\eta + \frac{\partial\Psi}{\partial\theta}\right) + \rho\frac{\partial\Psi}{\partial\mathbf{g}}\dot{\mathbf{g}} - \left[(\mathbf{T} + \boldsymbol{\sigma}')\mathbf{F}^{-\mathbf{T}} - \rho\frac{\partial\Psi}{\partial\mathbf{F}}\right]\dot{\mathbf{F}} + \frac{1}{\theta}\mathbf{q}.\mathbf{g} - \left(\boldsymbol{\sigma} - \frac{\partial\Psi}{\partial\boldsymbol{\psi}}\right)\dot{\boldsymbol{\psi}} \leq 0, \tag{22}$$

in which $\mathbf{g} \triangleq \boldsymbol{\nabla}\theta$.

This inequality must hold for any thermodynamic process$\{\rho, \rho', \boldsymbol{\sigma}, \boldsymbol{\sigma}', \mathbf{F}, \boldsymbol{\psi}, \theta, r\}$. Consequently, the following constraints must be satisfied.

$$\eta = -\frac{\partial\Psi}{\partial\theta},\ (23\text{-a})\quad \frac{\partial\Psi}{\partial\mathbf{g}} = 0,\ (23\text{-b})\quad \boldsymbol{\sigma} = \frac{\partial\Psi}{\partial\boldsymbol{\psi}},\ (23\text{-c})$$

$$(\mathbf{T} + \boldsymbol{\sigma}')\mathbf{F}^{-\mathbf{T}} = \rho\frac{\partial\Psi}{\partial\mathbf{F}},\ (23\text{-d})\quad \mathbf{q}.\mathbf{g} \leq 0,\ (23\text{-e})$$

These are constitutive constraints imposed by the second law of thermodynamics on the proposed ECM formulation. If we restrict ourselves to infinitesimal deformations, Eq. (23-d) transforms to:

$$(\mathbf{T} + \boldsymbol{\sigma}') = \frac{\partial\Psi}{\partial\mathbf{E}}\ , \tag{24}$$

in which **E** is the infinitesimal Lagrangian strain tensor.

4. IMPLEMENTATION

In the previous sections, the governing equations of the generalized continuum were laid down. Clearly, the resulting system is highly indeterminate and 31 independent additional equations are needed. These 31 additional equations consist of constitutive relations for T_{ij}, σ_{ij}, σ'_{ij}, q_i and η. Among these, η does not appear in other field equations and can be ignored. The classical Fourier's law of heat conduction can be adopted as the constitutive relations for q_i. The classical continuum mechanics theory can precisely be used in macro scales. Therefore, it is reasonable to assume that T_{ij}s obey the same relation and have the same material constants as for the classical stress in CCM.

$$T_{ij} = C_{ijkl}\varepsilon_{kl}, \tag{25}$$

where C_{ijkl} represents classical elasticity tensor. As mentioned earlier, two generalized stresses $\boldsymbol{\sigma}$ and $\boldsymbol{\sigma}'$are built-in in the continuum formulation in order to model the effects of the micro structure. The role of $\boldsymbol{\sigma}'$is to modify the macro stress in order to incorporate the microstructural effect (Eq. (15)). On the other hand, $\boldsymbol{\sigma}$ couples the equations of motion in two scales (Eqs. (15-a) and b). Accordingly, similar to MD simulations, even in a constant macro state the micro state evolves continuously in the present ECM formulation. The constitutive relations of $\boldsymbol{\sigma}$ and $\boldsymbol{\sigma}'$can be obtained using MD simulation results. It is

assumed that $\boldsymbol{\sigma}$ and $\boldsymbol{\sigma}'$ are functions of θ and ψ_{ij} explicitly and the dependence on macro kinematical variables such as **F** is modeled through the implicit dependency on θ. To present the constitutive relations for $\boldsymbol{\sigma}$ and $\boldsymbol{\sigma}'$, the first step is selecting a proper MD simulation cell. This MD cell is going to be a representative of the micro-element placed in each material point. This volume should be neither too small nor too large. In fact, the size of this volume should be about the validity border of the CCM. ψ_{ij}s are measures of severity of changes in micro deformation. They can be interpreted as the components of the micro strain tensor on the boundaries of the assumed microelement. Components of $\boldsymbol{\sigma}$ and $\boldsymbol{\sigma}'$ are some measures of action in micro space. $\boldsymbol{\sigma}'$can be regarded as a multiple of the local Virial stress tensor at the center of the MD domain (which is the place where micro and macro spaces are connected). Moreover, $\boldsymbol{\sigma}$ can be regarded as the Virial stress tensor on the boundary of the MD cell. This is shown schematically in Fig. 2. These two quantities are assumed to be presentable via different functions of ψ and θ. The adopted constitutive relations can be summarized as:

$$\eta = -\frac{\partial \Psi}{\partial \theta}, \text{ (26-a) } \mathbf{q} = -\mathrm{K}(\mathbf{E}, \theta)\mathbf{g}, \text{ (26-b) } \boldsymbol{\sigma} = \boldsymbol{\sigma}(\boldsymbol{\psi}, \theta), \text{ (26-c) } \boldsymbol{\sigma}' = \boldsymbol{\sigma}'(\boldsymbol{\psi}, \theta), \text{ (26-d)}$$

$$\mathbf{T} + \boldsymbol{\sigma}' = \frac{\partial \Psi}{\partial \mathbf{E}}. \text{ (26-e)}$$

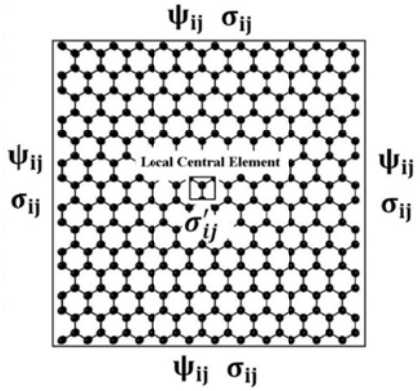

Fig. 2. Schematic representation of the micro element

To investigate the accuracy of the proposed model, it is used to predict the mechanical response of a graphene sheet. The Brenner potential is used to model the inter-atomic interactions. In order to find a proper size of microelement, several sizes have been investigated. The micro-elements are relaxed to their stress-free state then stretched in one direction. Resulting Virial stress in the loading direction on each element is compared with the corresponding expected value of Cauchy stress, which is the product of Young modulus of graphene in the loading direction and the corresponding strain value. Results are shown in Table 1. Accordingly, a volume consisting of 336 carbon atoms is considered as the micro-element. The multiplier factor of $\boldsymbol{\sigma}'$should be able to model the amplitude of local atomic motions. Analyzing the previous MD simulation results (cf. 23[23], Sec. 3.1) shows that the maximum/minimum of local Virial stresses regularly fluctuates above/below the Cauchy stress in the interval confined to one fifth of the value of macro stress which is predicted by CCM. Therefore, twenty percent of the Virial stress at LCE would be able to modify the local stresses. The MD model of the micro element can be relaxed at various temperatures. Hereinafter, the relaxed models are loaded by imposing the different components of $\boldsymbol{\psi}$ on their boundaries and $\boldsymbol{\sigma}$ and $\boldsymbol{\sigma}'$ can be obtained from MD. In the present work, $\boldsymbol{\sigma}$ and $\boldsymbol{\sigma}'$are evaluated at five and eight distinct values of θ and ψ_{ij} respectively as shown in Fig. 3. Using these values constitutive relations for $\boldsymbol{\sigma}$ and $\boldsymbol{\sigma}'$ in the form of two continuous functions can be constructed by adopting 3-cubic spline approximation.

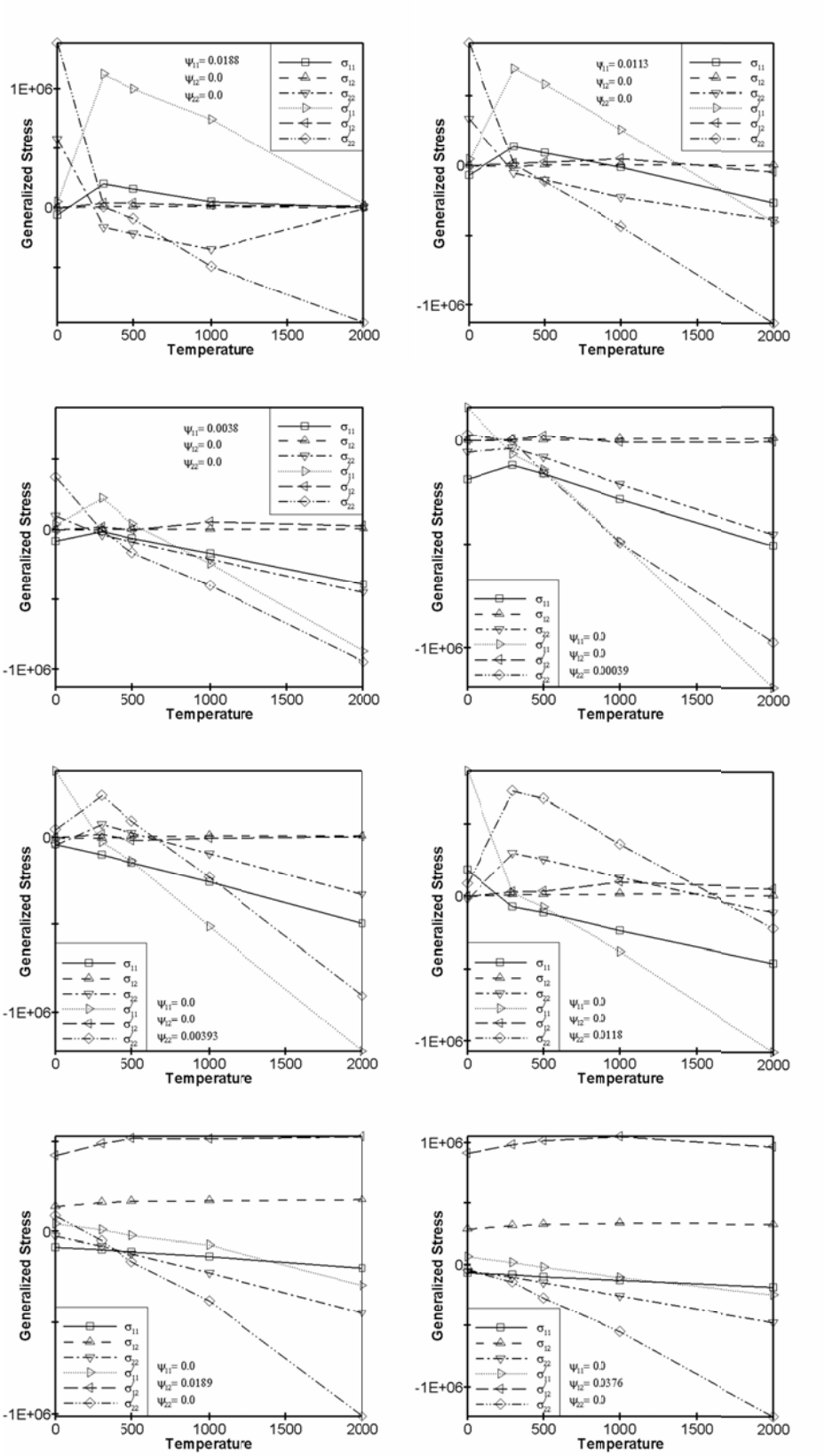

Fig. 3. Data used for obtaining constitutive relations for $\boldsymbol{\sigma}$and $\boldsymbol{\sigma}'$.Using these data two continuous functions can be constructed for $\boldsymbol{\sigma}$ and $\boldsymbol{\sigma}'$ by adopting 3-cubic spline approximation among these discrete values

Table 1. Selecting the proper size of microelement

Number of atoms	Virial stress ($\times 10^{10}$Pa)	Percentage error in comparison with the Cauchy stress
40	3.98	20.4
152	4.61	7.8
170	4.75	5
336	4.91	1.8
416	5.21	1.3

To examine the ability of the proposed model in predicting the behavior of nano-scale materials, this model is applied to a uniaxially loaded graphene sheet as shown schematically in Fig. 4. Assumed problem is a long graphene strip loaded in one direction without any heat source or heat flux. Therefore, it is reasonable to assume that the displacement components of the particles normal to the loading direction are zero. The general governing equation and constitutive laws of the extended continuum mechanics can be summarized as

$$\mathrm{E}\,\frac{\partial^2 \mathrm{u}}{\partial \mathrm{x}^2}+\frac{\partial \sigma'_{11}}{\partial \mathrm{x}}=\frac{\mathrm{D}}{\mathrm{Dt}}[(\rho+\rho')\dot{\mathrm{u}}]. \tag{27-a}$$

$$\frac{\mathrm{D}\varepsilon}{\mathrm{Dt}}=(\mathrm{T}_{11}+\boldsymbol{\sigma}'_{11})\dot{\mathrm{u}}_{1,1}+\sigma_{\mathrm{ji}}\dot{\psi}_{\mathrm{ij}}-\mathrm{q}_{1,1}. \tag{27-b}$$

$$\sigma_{11}=-\frac{\mathrm{D}}{\mathrm{Dt}}\left(\mathrm{I}_{1\mathrm{k}}\dot{\psi}_{1\mathrm{k}}\right). \tag{27-c}$$

$$\mathrm{q}=-\mathrm{k}\frac{\partial\theta}{\partial \mathrm{x}}. \tag{27-d}$$

$$\varepsilon=\rho \mathrm{C}\theta. \tag{27-e}$$

$$\rho'\triangleq\frac{\sum_{\alpha}^{\mathrm{N}}\mathrm{m}^{\alpha}}{\mathrm{V}'}. \tag{27-f}$$

where

$I_{jk}\triangleq\frac{\sum_{\alpha_2}^{\mathrm{N}_1}\mathrm{m}^{\alpha}\mathrm{X}_{\mathrm{j}}'^{\alpha}\mathrm{X}_{\mathrm{k}}'^{\alpha}}{\mathrm{V}'}$ and $\mathrm{u}=\mathrm{u}_0$ on ∂R. E and ρ represent the modulus of elasticity and mass density of the graphene sheet, respectively. These constants are used to model the macro state. On the other hand, ρ', I_{ij}, K and C stand for the micro mass density, micro inertia density, thermal conductivity and specific heat capacity of the graphene sheet, respectively. These parameters can be calculated by means of MD simulation. $\rho'$and I_{ij} (Eq. (10)) should be calculated at the reference configuration. We choose the fully relaxed model at 300 K as the reference configuration. Then, the following values are obtained by long time averaging of atomic positions of the fully relaxed MD model at 300 K.

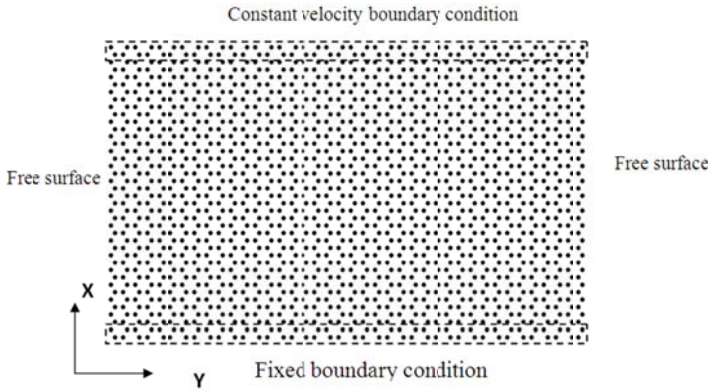

Fig. 4. Schematic representation of model used for MD simulation

$$I_{11} = 139.21 \times 10^{-16} \frac{\text{Kg}}{\text{Ang}}, \tag{28-a}$$

$$I_{12} = .0075 \times 10^{-16} \frac{\text{Kg}}{\text{Ang}}, \tag{28-b}$$

$$I_{22} = 149.977 \times 10^{-16} \frac{\text{Kg}}{\text{Ang}}, \tag{28-c}$$

$$\rho' = 59.3156 \frac{\text{kg}}{\text{Ang}^3}. \tag{28-d}$$

The values of K and C can be found in literature (e.g. [24]). We use $800 \frac{\text{W}}{\text{m.K}}$ and $1960 \frac{\text{J}}{\text{K.kg}}$ for K and C, respectively. According to the reported results in [25] and [26] and previous work by the authors [23], ρ and E are selected as $1000 \frac{\text{kg}}{\text{m}^3}$ and 0.6 TPa, respectively.

Obviously, the constants are completely in different orders of magnitude. It is more convenient to transform all equations to non-dimensional form. Utilizing the Buckingham π theorem, we select the following values as reference constants.$\theta_0 = 300\ K$, length of the graphene sheet$l_0 = 47$ Ang, mass of the carbon atom $m = 1.994 \times 10^{-26}$ kg and energy of the relaxed MD micro-volume at 300 K, $U_0 = 5.51782$ ev obtained by long time averaging of the energy of the relaxed micro volume. Substituting the scaled quantities into the governing Eq. (27) turns the problem into a set of non-dimensional coupled nonlinear differential equation shown below.

$$E^* \frac{\partial^2 u^*}{\partial x^{*2}} + \frac{\partial \sigma'^*_{11}}{\partial x^*} = \frac{D}{Dt^*}\left[\left(\rho^* + \rho'^*\right)\dot{u}^*\right], \tag{29-a}$$

$$\rho^* C^* \frac{\partial \theta^*}{\partial t^*} = \left(E^* \frac{\partial u^*}{\partial x^*} + \boldsymbol{\sigma'}^*_{11}\right)\dot{u}^*_{1,1} + \sigma^*_{ji} \frac{d\psi_{ij}}{dt^*} + k^* \frac{\partial^2 \theta^*}{\partial x^{*2}}, \tag{29-b}$$

$$\sigma^*_{11} = -\frac{D}{Dt^*}\left(I^*_{1k} \frac{d\psi_{1k}}{dt^*}\right), \tag{29-c}$$

with boundary conditions

$$u^* = u^*_0 \qquad \text{on } \partial R, \tag{29-d}$$

in which starred variables show the corresponding non-dimensional ones. The solution can be obtained by several numerical methods. Due to its generality and simplicity, we use the finite difference method. Furthermore, to get rid of difficulties, a trial and error procedure is used. In this procedure, we consider the temperature as a known trial function and obtain the resulting displacement function. In the next step, the obtained displacement function can be used to correct the previously used temperature function. This procedure is continued until the difference of the temperature values become negligible. The above mentioned procedure should be followed at each time step and the temperature and displacement can be obtained as functions of position and time. The MD simulation results and the CCM solution of the corresponding model are previously obtained by the authors [23].

5. RESULTS AND DISCUSSIONS

The displacement wave profiles for transmitted and reflected waves along the graphene sheet are compared in Figs. 5 and 6 respectively. Figure 5 shows the displacement wave shapes at $t = 0.045\ ps$ and $t = 0.1425\ ps$ as functions of x. The shape of the reflected displacement wave at $t = 0.375\ ps$ is depicted in Fig. 6. It can be seen that the predicted response by CCM and ECM are in good agreement with MD results. The difference between ECM response and MD simulation results in the wave front region can be a result of assumed model for heat transfer equation which is of parabolic type and has

infinite wave speed. Better results may be achieved by adopting the finite wave speed heat transfer model [27]. It is worth mentioning that, although there is some inaccuracy in the wave front region, the ECM has better accuracy in the affected region in which the actual physical response of material (e.g. crack growth morphology and failure mechanisms) is controlled. One of the important characteristics of the present ECM formulation over CCM setting is that this ECM formulation is able to mimic the instantaneous and local MD simulation results. More precisely, due to the concurrent connections with the MD results in the constitutive equations of σ and σ' the ECM responses fluctuate even in the case of constant external actions. This unique property is the characteristic of the present ECM formulation which up to the authors' knowledge is not seen in the other ECM formulations. The comparison between the scattered and reflected velocity wave shapes are shown in Figs. 7 and 8, respectively. Compared with CCM, the present ECM formulation can predict the local atomic motions. These local atomic vibration amplitudes are responsible for the local material failure [23]. As mentioned before, although ECM has acceptable accuracy in affected region, the wave front profile of ECM solution shows incorrect shape which is probably caused by infinite wave speed characteristic of heat transfer equation. As simulation advances in time, ECM model in which the temperature effects are included shows a better output and can effectively follow the MD results. It is worth mentioning that even in the MD simulation, the exact prediction of atomic movements is not possible and two MD runs with the same external inputs will show different instantaneous outputs. However, the order of fluctuation of outputs is the same, of course. In the same way, the instantaneous results of the present ECM formulation are expected to fluctuate in the same order as the MD simulation ones. The shapes of strain wave are compared in Figs. 9 and 10. The well-known phenomenon of duplication of the amplitude of the reflected strain wave which was seen in previous researches [23] can also be correctly predicted by the newly presented ECM formulation. Furthermore, since atomic behavior is modeled with continuous field equations, the computational time is in the order of CCM while the MD simulation for sizes larger than one micro-meter is partially intractable, even with the today's computers.

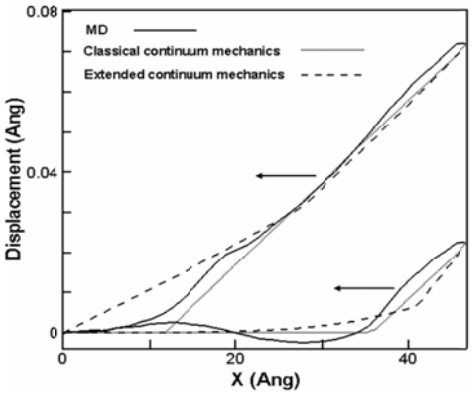

Fig. 5. Comparison between displacement values obtained from CCM and ECM with MD results at $t = 0.045\ ps$(right curves) and $t = 0.1425\ ps$(left curves)

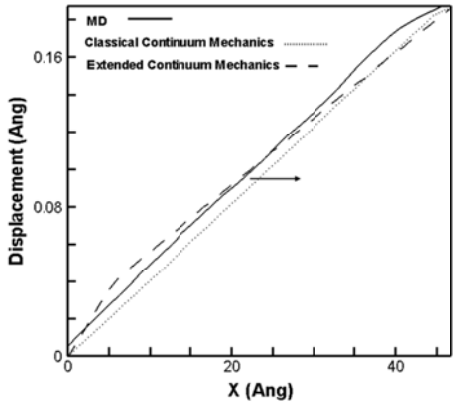

Fig. 6. Comparison between shapes of the reflected displacement wave obtained from MD simulation with those predicted by CCM and ECM at the same time

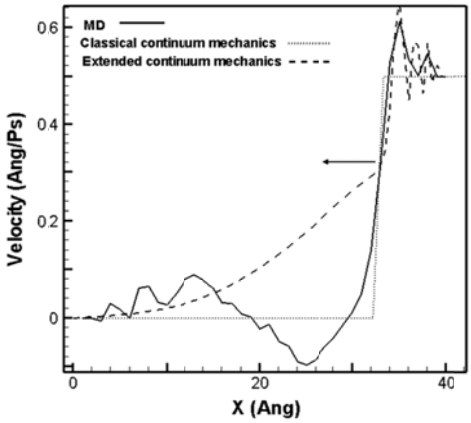

Fig. 7. Comparison between shapes of velocity waves obtained from MD simulation with those predicted by CCM and ECM

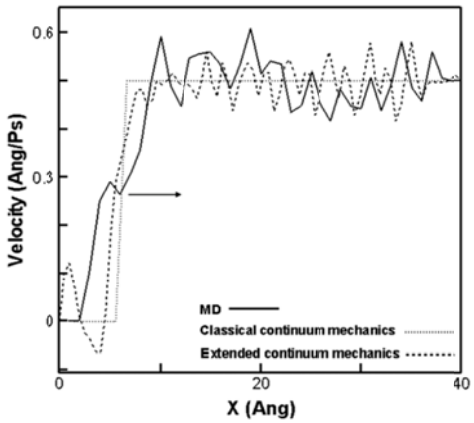

Fig. 8. Comparison between shapes of reflected velocity waves obtained from MD simulation with those predicted by CCM and ECM

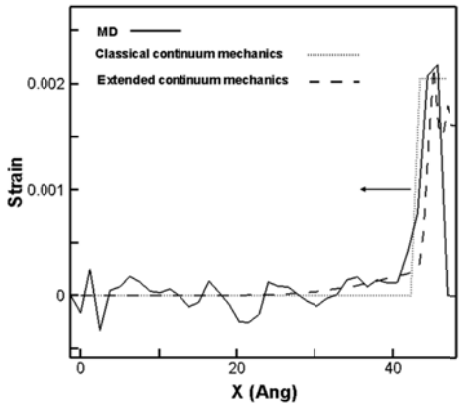

Fig. 9. Comparison between shapes of strain waves obtained from MD simulation with those predicted by CCM and ECM

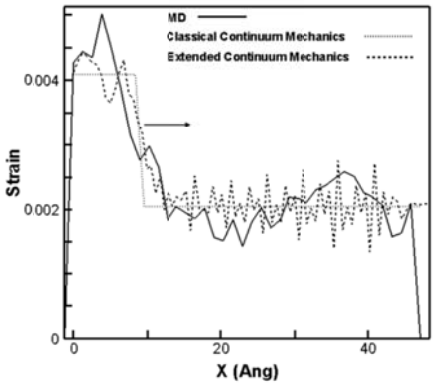

Fig. 10. Comparison between shapes of reflected strain waves obtained from MD simulation with those predicted by CCM and ECM

6. CONCLUDING REMARKS

A new extended continuum mechanics model together with all field equations and general framework for their application was presented. To validate the present ECM model, the model response was evaluated. The assumed sample problem was a planar graphene sheet loaded in one direction. The response obtained by ECM was compared with MD and CCM results. This comparison showed that the present ECM model has acceptable performance in predicting the local instantaneous atomic motions. The proposed framework can be used to obtain the response of a dynamically evolving system of material particles and can effectively predict the MD results.

REFERENCES

1. Eringen, A. C. (1998). *Microcontinuum Field Theories I. Foundations and Solids*. Springer-Verlag, New York.
2. Cosserat, E. & Cosserat, F. (1909). *Theorie des Corps Deformables*. Paris: Hermannet Fils.
3. Voigt, W. (1887). Theoretische Studienüber die Elasticität sverhältnisse der Krystalle. *Abh. Kgl. Ges. Wiss. Göttingen, Math. Kl*., Vol. 34, pp. 3–51.
4. Mariano, P. M. (2002). Multifield theories in mechanics of solids. *Adv. Appl. Mech.*, Vol. 38.
5. Mariano, P. M. & Stazi, F. L. (2005). Computational aspects of the mechanics of complex materials. *Arch. Comput. Meth. Engng*.,Vol. 12, Issue 4, pp. 391-478.
6. Toupin, R. A. (1962). Elastic materials with couple-stresses. *Arch. Ration. Mech. An*., Vol. 11, No. 1, pp. 385-414.

7. Mindlin, R. D. (1964). Microstructure in linear elasticity. *Arch. Ration. Mech. An*., Vol. 16, Issue 1, pp. 51 – 78.
8. Eringen, A. C., Suhubi, E. S. (1964). Nonlinear theory of simple microelastic solids- I. *Int. J. Eng. Sci.,* Vol. 2, Issue 2,pp. 198 – 203.
9. Eringen, A. C., Suhubi, E. S. (1964). Nonlinear theory of simple microelastic solids- II. *Int. J. Eng. Sci.,* Vol. 2, pp. 389-404.
10. Green, A. E. & Rivlin, R. S. (1964). Simple force and stress multipoles. *Arch. Ration. Mech. An*., Vol. 16, Issue 5, pp. 325-353.
11. Green, A. E. & Rivlin, R. S. (1964). Multipolar continuum mechanics. *Arch. Ration. Mech. An.,* Vol. 17, Issue 2, pp. 113-147.
12. Chen, Y., Lee, J. D. & Eskandarian, A. (2004). Atomistic viewpoint of the applicability of microcontinuum theories, *Int. J. Solids Struct.*, Vol. 41, pp. 2085–2097.
13. Chen, Y., Lee, J. D. & Eskandarian, A. (2003). Examining the physical foundation of continuum theories from the viewpoint of phonon dispersion relation. *Int. J. Eng. Sci.*, Vol. 41, pp. 61–83.
14. Chen, Y. & Lee, J. D. (2003). Connecting molecular dynamics to micromorphic theory. (I). Instantaneous and averaged mechanical variables. *Physica A: Statistical Mechanics and its Applications*, Vol. 322, pp. 359 – 376.
15. Chen, Y. & Lee, J. D. (2003). Connecting molecular dynamics to micromorphic theory. (II). Balance laws, *Physica A: Statistical Mechanics and its Applications*, Vol. 322, pp. 377 – 392.
16. Gnanasundarajayaraja, B., Selvakumar, N. & Murugesh, R. (2014). Characterisation, testing and software analysis of al-wc nano composites. *IJST, Transactions of Mechanical Engineering*, Vol. 38, No. M1, pp. 105-117.
17. Ansari, R., Rouhi, H. & Arash, B. (2013). Vibrational analysis of double-walled carbon nanotubes based on the nonlocal donnell shell theory via a new numerical approach. *Iranian Journal of Science & Technology, Transactions of Mechanical Engineering*, Vol. 37, No. M2, pp. 91-105.
18. Xiaowei, Z., Xianqiao, W., James, D. L. & Yajie, L. (2011).Multiscale modeling of nano/micro systems by a multiscale continuum field theory. *Comput. Mech.*, Vol. 47, pp. 205–216.
19. Fafalis, D. A., Filopoulos, S. P. & Tsamasphyros, G. J. (2012). On the capability of generalized continuum theories to capture dispersion characteristics at the atomic scale. *Eur. J. Mech. A-Solid*, Vol. 36, pp. 25-37.
20. Öchsner, A. & Shokuhfar, A. (2013). *New frontiers of nanoparticles and nanocomposite materials, Novel Principles and Techniques, Advanced Structured Materials*. Vol. 4, Springer Heidelberg New York Dordrecht London.
21. Tapasztó1, L., Dumitric˘a, T., Kim, S. J., Nemes-Incze, P., Hwang, C. & P. Biró1 L. (2012). Breakdown of continuum mechanics for nanometre-wavelength rippling of graphene, *Nature Physics*, Vol. 8, pp. 739-742.
22. Coleman, B. & Noll, W. (1963). The Thermodynamics of Elastic Materials with Heat Conduction and Viscosity. *Arch. Ration. Mech. An*., Vol. 13, pp. 167-178.
23. Habibi, S. E., Farid, M. & Kadivar, M. H. (2010). Continuum mechanics ability to predict the material response at atomic scale. *Comp. Mater. Sci.*, Vol. 48, pp. 372–380.
24. Jauregui, L. A., Yue, Y. N., Sidorov, A. N., Hu, J. N., Yu, Q. K., Lopez, G., Jalilian, R., Benjamin, D. K., Delk, D. A., Wu, W., Liu, Z. H., Wang, X. W., Jiang, Z., Ruan, X. L., Bao, J. M., Pei, S. S. & Chen, Y. P. (2010). Thermal transport in graphene nanostructures: experiments and simulations. *ECS Trans*., Vol. 28, Issue 5, pp. 73-83.
25. Pierson, H. O. (2004). *Handbook of carbon, graphite, diamond, and fullerenes: Properties, Processing and Applications*. William Andrew Publishing/Noyes.
26. Jenkins, G. M. & Kawamura, K. (1976). *Polymeric Carbons*, Cambridge Univ. Press, Cambridge UK.
27. Ignaczak, J. & Ostoja-Starzewski, M. (2010). *Thermoelasticity with Finite Wave Speeds*. Oxford University Press.